



Investigation of Recently Introduced Diffusion Coefficient Generation Methods

András Szabolcs Ványi

Budapest University of Technology and Economics
Műegyetem rkp. 3.
1111, Budapest, Hungary
vanyi.andras@reak.bme.hu

Mathieu Hursin

Paul Scherrer Institut
Forschungsstrasse 111
5232, Villigen, Switzerland
mathieu.hursin@psi.ch

Szabolcs Czifrus

Budapest University of Technology and Economics
Műegyetem rkp. 3.
1111, Budapest, Hungary
czifrus@reak.bme.hu

ABSTRACT

The multigroup diffusion theory is one of the most widely used methods for deterministic reactor core calculations. In this approach the angular dependence of the neutron flux and the scattering kernel is expanded with spherical harmonics to the P_1 order. The P_1 scattering matrix is then used to generate a scalar quantity for each energy group, the group diffusion coefficient. As the entire linearly anisotropic angular dependence is represented in the group diffusion coefficients, the accuracy of the diffusion calculations highly depends on how those coefficients are determined. Recently, two approaches were introduced by researchers of the Massachusetts Institute of Technology to produce accurate diffusion coefficients using Monte Carlo codes: the Neutron Leakage Correction method [1] and the Cumulative Migration Method [2].

After providing a brief overview of the methods, a parametric study is carried out in this paper where the performance of those approaches in terms of power distribution and multiplication factor of the associated diffusion calculations is assessed. For this purpose, 1D and 2D models based on the specifications of the DIMPLE benchmark [3] are used. The Monte Carlo simulations for group constant generation and reference calculations were carried out by the Serpent 2 code, while the deterministic calculations were performed by the PARCS nodal diffusion code.

1 INTRODUCTION

Diffusion codes are based on the multigroup diffusion equation (Eq. 1), which can be derived from the low-order P_1 equations (for details see the textbooks [4, 5]).

$$\frac{1}{v} \frac{\partial \Phi(\mathbf{r}, E, t)}{\partial t} = \nabla (D(\mathbf{r}, E) \nabla \Phi(\mathbf{r}, E, t)) - \Sigma_t(\mathbf{r}, E) \Phi(\mathbf{r}, E, t) + Q_0(\mathbf{r}, E, t) \quad (1)$$

In Eq. 1 Φ is the scalar flux, v the neutron velocity, Σ_t the total cross-section, Q_0 the isotropic source term and D the diffusion coefficient which is usually defined as:

$$D(\mathbf{r}, E) = \frac{1}{3} \left(\Sigma_t(\mathbf{r}, E) - \frac{\int_0^\infty \Sigma_{s1}(\mathbf{r}, E' \rightarrow E) \mathbf{J}(\mathbf{r}, E', t) dE'}{\mathbf{J}(\mathbf{r}, E, t)} \right)^{-1} = \frac{1}{3\Sigma_{tr}(\mathbf{r}, E)}, \quad (2)$$

where Σ_{tr} is the so-called transport cross-section. In Eq. 2 the term containing the current \mathbf{J} and its integral is unknown prior to the calculations, thus, to compute D an approximation needs to be introduced. As the entire linearly anisotropic contribution of the scattering matrix is represented in the diffusion coefficient, to obtain the best possible angular treatment the assumptions made for its generation must be well-founded and well-suited for the given problem. Recently, two novel Monte Carlo based approaches were introduced [1, 2]. The goal of this paper is to present a parametric study related to these new methods and to assess their performance through a brief numerical study.

In Section 2 a short overview is given of two traditional and the two novel methods of diffusion coefficient generation. Section 3 comprises of the parametric study of the so-called transport correction curves. Finally, Section 4 presents a numerical study which assesses the presented diffusion generation methods in terms of power distribution and multiplication factor.

2 DIFFUSION COEFFICIENT GENERATION METHODS

Over the years several approximations have been developed to appropriately generate diffusion coefficients and transport cross-sections [1, 2, 4, 6, 7, 8]. This section briefly describes two traditional deterministic and two newly introduced Monte Carlo based approaches. For simplicity, the approximations are presented for the transport cross-section (see Eq. 2). However, it is important to note (as it was recently emphasized in several papers [1, 9, 10]) that flux-weighted energy condensation should be done according to the diffusion coefficient and not the transport cross-section.

2.1 Out-scatter approximation

The out-scatter approximation assumes that the linearly anisotropic term of the scattering matrix does not contribute to the energy transfer, therefore it can be approximated as:

$$\Sigma_{s1}(\mathbf{r}, E' \rightarrow E) \approx \Sigma_{s1}(\mathbf{r}, E) \delta(E' - E). \quad (3)$$

Substituting Eq. 3 to Eq. 2 results in the out-scatter approximation of the transport cross-section:

$$\Sigma_{tr}(\mathbf{r}, E) = \Sigma_t(\mathbf{r}, E) - \int_0^\infty \Sigma_{s1}(\mathbf{r}, E \rightarrow E') dE'. \quad (4)$$

As the model is relatively easy to implement, it is used by numerous lattice physics codes (e.g. SCALE/XSDRNPM, Serpent 2, etc.). The assumption is generally considered to be valid while absorption is weak and anisotropic scattering is not significant [5].

2.2 Flux-limited approximation

As an effort to treat the effect of anisotropic scattering in reactor systems Pomraning introduced the flux limited diffusion theory [7], which assumes that the magnitude of the current can not be greater than the scalar flux. The related theory for the calculation of transport cross-section (Eq. 5) uses scalar flux weighting instead of current weighting.

$$\Sigma_{tr}(\mathbf{r}, E) = \Sigma_t(\mathbf{r}, E) - \frac{\int_0^\infty \Sigma_{s1}(\mathbf{r}, E' \rightarrow E) \Phi(\mathbf{r}, E', t) dE'}{\Phi(\mathbf{r}, E, t)} \quad (5)$$

2.3 Neutron Leakage Conservation method

In 2013 Herman [1] introduced a method which is often referred to as the Neutron Leakage Conservation (NLC) method. Instead of explicitly approximating Eq. 2, for a given material the NLC method takes pre-calculated reference $\Sigma_{tr,g}^{REF}/\Sigma_{t,g}^{REF}$ ratios from a homogeneous 1D finite slab fixed-source problem for every g energy group and multiplies them with the appropriate group macroscopic total cross-section of the given case (Eq. 6). The result is a transport cross-section, which inherently contains the anisotropy of the scattering.

$$\Sigma_{tr,g} = \left[\frac{\Sigma_{tr,g}^{REF}}{\Sigma_{t,g}^{REF}} \right] \Sigma_{t,g} \quad (6)$$

To compute the reference cross-section ratios, let us consider a finite, homogeneous 1D slab with a length of W , bounded by vacuum on both sides. For this simple case multigroup diffusion theory yields Eq 7.

$$J_g(a) - J_g(-a) = D_g B_g^2 \Phi_g W \quad (7)$$

It can be shown that for this simple case of slab the buckling (B) is group-independent. If the current is tallied at $\pm a$ and the scalar flux is integrated for $x \in [-a, a]$ with a Monte Carlo code (such as Serpent, OpenMC, etc.) the group diffusion coefficients can be easily obtained from Eq. 7.

According to [9] since the 1970s the CASMO lattice physics code has been using a similarly constructed P_1 flux spectrum for treating the anisotropic scattering of hydrogen.

2.4 Cumulative Migration Method

The Cumulative Migration Method (CMM) is a new Monte Carlo based approach introduced by Liu in 2016 [2]. Its essential quantity is the migration area which can be defined in one-group diffusion theory as:

$$M^2 = \frac{D}{\Sigma_a} = \frac{1}{6} \bar{r}^2, \quad (8)$$

where Σ_a is the one-group absorption cross-section and \bar{r}^2 the average square of crow flight length of a neutron between its initial and final positions. In [11] the concept of *partial migration area* was introduced as:

$$M^2(E > E_g) = \frac{D(E > E_g)}{\Sigma_r(E > E_g)}, \quad (9)$$

where Σ_r is the removal cross-section. Taking an arbitrary $\Gamma = \{1, 2, \dots, g, \dots, G\}$ group structure, a partial migration area can be defined for all $[E_{max}, E_g]$ intervals, creating a new cumulative

group structure (denoted by upper index “c”) for each of which Eq. 9 applies. By tallying the particle path and directions, the cumulative migration areas can be computed from Eq. 10 and the group diffusion coefficients can be calculated from Eq. 11.

$$(M_g^c)^2 = \frac{1}{6}(\overline{r_g})^2 = \frac{D_g^c}{\Sigma_{r,g}^c} \quad (10) \quad D_g^c = \frac{\sum_{g'=1}^g D_{g'} \Phi_{g'}}{\sum_{g'=1}^g \Phi_{g'}} \quad (11)$$

According to [9, 11, 12], for infinite medium problems CMM can calculate the exact diffusion coefficients defined by Eq. 2. However, due to the fundamental concept of the migration area the application of the method for finite, heterogenous systems is not resolved, yet. For such cases, identically to the technique used with the NLC method, the authors recommend the computation and application of Σ_{tr}^g/Σ_t^g transport correction ratios (TCRs) from homogenous fixed source problems where CMM is applicable.

3 PARAMETRIC TCR STUDY

The goal of this parametric study is to compare the TCR curves of different methods, cross-section libraries and materials. As a tool to generate group constant data for the analysis the Serpent 2 Monte Carlo code was chosen with ENDF/B-VII.0 format data libraries. Beyond the general particle transport and group constant generation capabilities, the used code version (Serpent 2.1.31) is also fitted with the ability to generate diffusion coefficient based on the CMM method. Four common reactor materials were chosen for the tests: light water, beryllium, graphite and steel (identical composition to [3]).

3.1 Known guidelines for TCR curve generation

Regarding the NLC method, it is already stated in [1] that edge effects need to be avoided by appropriately choosing the sub-region of the integration.

For the CMM method the only known constraint is that the Monte Carlo simulation must be performed in infinite geometries with appropriate source. It was shown in [11] (and demonstrated for an infinite medium of hydrogen), that TCR curves generated by CMM are not sensitive to material density or the size of the Monte Carlo geometry either.

3.2 Comparison of TCR curves of NLC and CMM methods

For this parametric study a number of TCR curves were generated by both NLC and CMM methods for all four examined materials using SCALE 238-group structure [13] and ENDF/B-VII.0 libraries of 300 K supplemented with the corresponding $S(\alpha,\beta)$ data in the case of water and graphite.

NLC slab length was varied between 10 cm and 1000 cm, for each case the tallied sub-slab was the central 20%, 40%, 60% and 80% of the full slab length. In the case of water, TCR curves were generated for 0.5 g/cm³ and 1.5 g/cm³ density slab as well. Each calculation was carried out using appropriately buckled cosine shaped source with ²³⁵U fission spectrum.

CMM based TCR curves were generated for 10 cm, 100 cm and 1000 cm wide slabs with reflective boundary criteria. In the case of water 0.5 g/cm³ and 1.5 g/cm³ densities and different source shapes (periodic plane, cosine or homogeneous) with ²³⁵U fission spectrum were examined as well.

Based on the analysis and comparison of the curves the following conclusions could be drawn:

1. Supplementing [11], a TCR curve generated for a given material using CMM is independent of the infinite Monte Carlo slab length, the density of the material and the shape of the fixed source.
2. By increasing the NLC slab length the TCR curves converge to a reference solution. For a given slab length by decreasing the sub-slab length the solution improves to the reference curve. Both increasing the overall slab length and decreasing the sub-slab length make it necessary to run more neutrons to achieve the same Monte Carlo statistics.
3. The material density used in the NLC method does not affect the validity of the method, however, to achieve the same accuracy with decreased density, the slab length needs to be increased.
4. For all four investigated materials the TCR curves of the CMM method match perfectly the converged reference TCR curves generated by the NLC method within the Monte Carlo statistical uncertainty. Thus, after [11], it is demonstrated that NLC and CMM provides the exact same solution for the most commonly used neutron scattering materials.
5. To obtain a TCR curve of a given precision CMM is considerably faster than NLC which is burdened by the relatively high statistical uncertainty of the current tallies. Thus, for the rest of the paper only the CMM method will be used for TCR curve generation.

Due to the limited space the TCR curves generated by the NLC and CMM methods are only presented for water and steel (see Figures 1 and 2, respectively). TCR values for energies below 10^{-9} MeV for water, 10^{-7} MeV for steel and above 10 MeV for both materials are not shown due to the large associated Monte Carlo uncertainty.

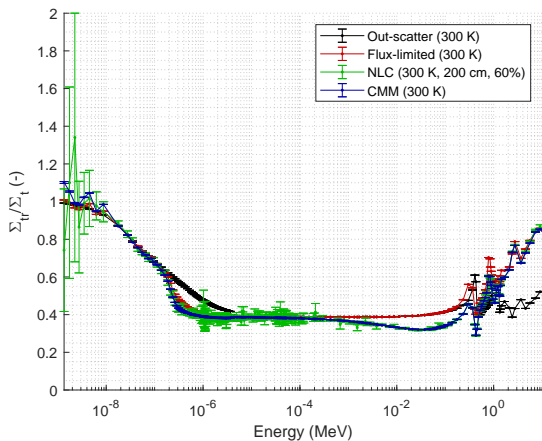


Figure 1: TCR curves of various methods for water

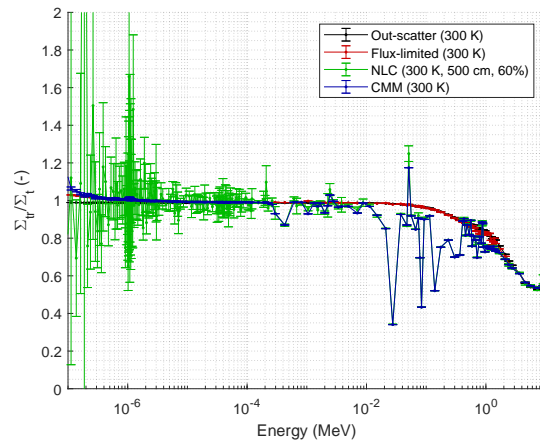


Figure 2: TCR curves of various methods for steel

3.3 Cross-section library dependence

TCR curves were generated with the CMM method for all four investigated materials for 300 K, 600 K and 900 K temperatures first using ENDF/B-VII.0, then JEFF3.1.1 libraries. For a given material and temperature the ENDF and JEFF curves agree within a few standard deviations between 10^{-7} MeV and 10 MeV, while at lower energies significant deviations can be observed (see relative difference¹ in % for water in Figure 3). For a given material the curves

¹ $(\text{ENDF} - \text{JEFF})/\text{ENDF} \cdot 100$

are in good agreement except for thermal energies where the curves part significantly from each other due to the shift in the thermal Maxwell-Boltzmann spectra (see Figure 4).

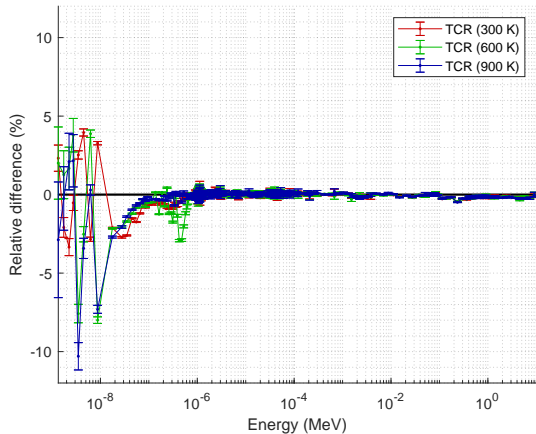


Figure 3: Relative difference of JEFF and ENDF water TCR curves generated by the CMM method

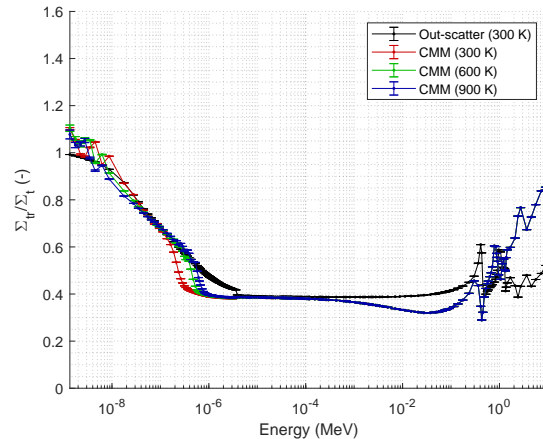


Figure 4: Water TCR curves for different ENDF temperature libraries generated by the CMM method

4 NUMERICAL STUDY

To assess the performance of the methods 1D and 2D models of the DIMPLE benchmark [3] were chosen as reference problem. The 2D model is identical to the one quarter of the DIMPLE S06B benchmark with the whole geometry being 3×10.0056 cm long in x and y direction as well (see Figure 6). The 1D problem is a 2×10.0056 cm long slab and consists of one fuel and one moderator (baffle and water) region of the same dimensions and materials as the original 2D problem (1D along the homogenized fuel-moderator axis, see Figure 5). For both models reflective boundary condition was applied at the edges.

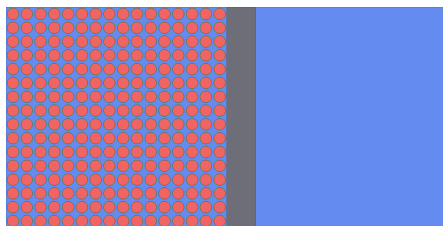


Figure 5: 1D model geometry

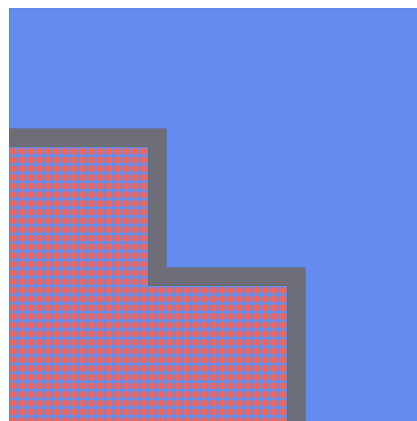


Figure 6: 2D model geometry

For both 1D and 2D models four geometries were created with the baffle material being water, graphite, beryllium and steel. Group constants were generated for CASMO 2-group and CASMO 70-group structures (with default micro multi-group structure [13]) by the Serpent 2 program using the full geometry (*full-core approach*) and ENDF/B-VII.0 libraries evaluated at 300 K. Diffusion coefficients were calculated with the traditional out-scatter (default method)

and flux-limited approaches as well as with the novel CMM transport correction method (only applied to the four investigated materials). The deterministic calculations were carried out with the PARCS nodal diffusion code (version 3.3.1), while the appropriate cross-section files were prepared with the GENPMAXS module (version 6.2). The results are assessed by the multiplication factor, the power distribution and the volume integrated flux distribution RMS errors² while taking the Serpent results as reference. Due to the lack of space, in this paper, only the more relevant 2D case results for water and steel baffle are presented (see Table 1).

Table 1: Calculation results of the 2D DIMPLE benchmark

	Multiplication factor		Power RMS (%)	Flux RMS (%)	
	k_{eff}	$(k_{\text{eff}} - k_{\text{ref}}) \times 10^5$		Fast	Thermal
<i>Water baffle</i>					
Out-scatter	1.09126	-639	0.893	0.505	6.293
Flux-limited	1.10490	725	2.611	0.677	2.101
TCR (CMM)	1.09924	159	2.323	0.580	4.010
<i>Steel baffle</i>					
Out-scatter	1.09249	778	7.117	2.454	6.559
Flux-limited	1.10037	1566	7.024	2.292	5.421
TCR (CMM)	1.09479	1008	6.740	2.232	5.890

In these cases the surprisingly good performance of the out-scatter approximation is probably due to error cancellation (see power distribution RMS). It can be seen from Table 1 that it is really difficult to draw a general conclusion on performance of the models based on the performed calculations. The most likely reason behind this is the complexity of the chosen benchmark problem from the point of view of the diffusion coefficient generation. The method to be applied for a given homogenization region should always be carefully handpicked based on the given materials along with the estimated flux and current spectra. Using the same diffusion coefficient generation method for a realistic full-core problem will probably not result in the best achievable flux and/or power distribution. In parallel to this work a journal paper is being prepared by the same authors in which the issue of choosing appropriate diffusion coefficient is investigated through different benchmark problems.

5 SUMMARY

In this paper, a parametric and a brief numerical study was presented of two recently introduced Monte Carlo based diffusion coefficient generation methods (NLC and CMM). The goal of the parametric study was to investigate the material, cross-section library, temperature, density etc. dependence of the resulting transport correction ratio (TCR) curves. Based on the calculation results TCR generation guidelines were formulated and the equivalence of the NLC and CMM TCR curves was demonstrated once again. The comparative numerical study showed that none of the presented methods are ultimately better or worse than the other. The diffusion

$${}^2RMS = \sqrt{\frac{1}{N} \sum_{i=1}^N (x_i - x_{ref,i})^2}$$

coefficient generation method applied to a given homogenization region should be specifically chosen based on the problem circumstances (material, spectra). A continuation of this work is being prepared by the authors in the form of a journal paper.

REFERENCES

- [1] B. R. Herman, B. Forget, K. Smith, B. N. Aviles, “Improved diffusion coefficients generated from Monte Carlo codes.”, Technical report, American Nuclear Society, 555 North Kensington Avenue, La Grange Park, IL 60526 (United States), 2013
- [2] Z. Liu, K. Smith, B. Forget, “A Cumulative Migration Method for Computing Rigorous Transport Cross Sections and Diffusion Coefficients for LWR Lattices with Monte Carlo”, *PHYSOR*, pp. 2915–2930, 2016
- [3] D. Hanlon, S. Assurancet, “Light Water Moderated and Reflected Low Enriched Uranium (3 wt.% ^{235}U) Dioxide Rod Lattices”, NEA/NSC/DOC(95)03/IV, Vol. 4, LEU-COMP-THERM-055, 2002
- [4] J. J. Duderstadt, L. J. Hamilton, “Nuclear Reactor Analysis”, John Wiley & Sons Inc., 1976
- [5] R. J. Stamm’ler, M. J. Abbate, “Methods of Steady-State Reactor Physics in Nuclear Design”, vol. 111., Academic Press London, 1983
- [6] G. I. Bell, G. E. Hansen, H. A. Sandmeier, “Multitable Treatments of Anisotropic Scattering in S_N Multigroup Transport Calculations”, *Nuclear Science and Engineering*, 28:3, 376-383, DOI: 10.13182/NSE67-2, 1967
- [7] G. C. Pomraning, “Flux-Limited Diffusion Theory with Anisotropic Scattering”, *Nuclear Science and Engineering*, 86:4, 335-343, DOI: 10.13182/NSE84-A18634, 1984
- [8] A. Yamamoto, Y. Kitamura, Y. Yamane, “Simplified Treatments of Anisotropic Scattering in LWR Core Calculations”, *Journal of Nuclear Science and Technology*, 45:3, 217-229, DOI: 10.1080/18811248.2008.9711430, 2008
- [9] K. Smith, “Nodal diffusion methods and lattice physics data in LWR analyses: Understanding numerous subtle details”, *Progress in Nuclear Energy*, Vol. 101, pp. 360-369, 2017
- [10] J. Leppänen, M. Pusa, E. Fridman, “Overview of methodology for spatial homogenization in the Serpent 2 Monte Carlo code”, *Annals of Nuclear Energy*, Vol. 96, pp. 126-136, 2016
- [11] Z. Liu, K. Smith, B. Forget, J. Ortensi, “Cumulative migration method for computing rigorous diffusion coefficients and transport cross sections from Monte Carlo”, *Annals of Nuclear Energy*, Vol. 112, pp. 507-516, 2018
- [12] Z. Liu, G. Giudicelli, K. Smith, B. Forget, “Conservation of migration area by transport cross sections using Cumulative Migration Method in deterministic heterogeneous reactor transport analysis”, *Progress in Nuclear Energy*, Vol. 127, 2020
- [13] https://serpent.vtt.fi/mediawiki/index.php/Pre-defined_energy_group_structures
[Cited: 2021/08/11 12:30]